Robust Si-Based Membranes for Fluid Control in Microbatteries Using Superlyophobic Nanostructures

Victor A. Lifton, *Member, IEEE*, and Steve Simon, *Member, IEEE*

***Abstract*—Mechanically robust superhydrophobic Si-based membranes are described. The membranes are prepared using microelectromechanical-systems-type processing and implement "nanonail" design features that enable superlyophobic (also called omniphobic, superolephobic) behavior. A variety of low- and high-surface-tension liquids are repelled by such porous membranes without liquid penetrating into the pores of the membrane. Electrowetting transitions have been successfully implemented as a way to demonstrate electrically triggered and tunable permeability of the structures. Long-term stability of the hydrophobic coatings based on fluoropolymers has been evaluated using contact angle measurements. Among those, Teflon-based coatings tend to show the best survivability in aqueous and organic electrolytes for periods longer than 200 days of continuous exposure at room temperature and at 60 °C. Such robust membranes are currently used in reserve microbattery technology and microfluidic devices and, potentially, could enable other applications involving fluid separation, fuel cells, and filtration. [2010-0147]**

***Index Terms*—Battery, electrowetting, membrane, microelectromechanical systems (MEMS) processing, porous, superhydrophobic.**

I. Introduction

FABRICATION and processing of superhydrophobic surfaces is, by now, a well-established research direction in the surface science and nanotechnology fields [1]–[6]. In fact, it is at the intersection of these two fields that superhydrophobic materials and properties associated with this state are found. Many parallels to the structures can be found in nature, such as superhydrophobic surfaces and structures developed in the course of evolution on lotus leafs, beetles, butterflies, and others [7].

The subject of superhydrophobicity is wide ranging and includes the art of making such materials, nanofabrication and testing and, more recently, commercialization of products that include superhydrophobic properties [2], [8]–[13]. The superhydrophobic state is typically characterized by a very high contact angle, free-moving (or so called "rolling" ball) droplets, and very low contact angle hysteresis. "Sticky" superhydrophobic surfaces have also been presented in literature [14], [15]. Concurrently with the superhydrophobic materials (characterized by the high contact angle of the aqueous high-surface-tension liquids), omniphobic (also referred to as superoleophobic, superlyophibic) materials have recently been described [11], [16]. These are highly repelling materials against not only aqueous high-surface-tension liquids, but also against low-surface-tension organic liquids such as oils and alcohols.

In a regular superhydrophobic material, a droplet of liquid is supported by the very tips of the nano- and microstructures required to obtain the superhydrophobic behavior. Since superhydrophobicity is a surface phenomenon, properties of the underlying materials (bulk or nanostructured as well) play no role in the observation of the effect. Consequently, most of the superhydrophobic materials consist of a bulk material (e.g., Si wafer, metal plate, polymer sheet) that are etched on the surface and/or coated with nanoparticles to create nanostructures on its surface. While this approach has its merits in cases where only the surface of the material will come in contact with the fluid, we expanded this approach and imagined situations where the liquid may be required to flow through the bulk of the superhydrophobic material, and where a switchable or controllable permeability of the superhydrophobic material may assist in fluid separation, filtration, and other frequently employed microfluidic techniques. By controllable permeability, we envisioned the ability of a porous material to repel the liquid on its surface, and yet on command, allow the liquid to fill the pores of the material to reach the opposite end and, under the right conditions, to exit the pores. That is to say, a complete transfer of the liquid from the top to the backside of the porous material throughout its thickness can be achieved. On the other hand, controllable permeability may also manifest itself by allowing liquids of certain (low) surface tension to go through the membrane, while repelling the high-surface-tension liquids, thus, preventing them from going through the porous substrate. The design and fabrication of mechanically stable Si-based membranes with controllable permeability is the subject of this paper.

Previously, we reported on the design and fabrication of thin silicon-on-insulator (SOI)-based superhydrophobic and superlyophobic membranes [Fig. 1(a)] [11], [17]. We demonstrated controllable permeability in 30-μm thick porous silicon membranes by implementing electrowetting transitions. With a pool of liquid placed on such tunable membrane, and by applying a short voltage pulse, the balance of surface energies at the "solid–liquid–vapor" interfaces was altered and the liquid began to spread and permeate through the thickness of the membrane. With a layer of hydrophilic material (acting as a wick) placed directly under the bottom surface of the membrane, complete transfer of the liquid throughout the membrane's thickness was demonstrated [Fig. 1(c)]. In this approach, the SOI device

Manuscript received May 18, 2010; revised September 13, 2010; accepted October 17, 2010. Portions of this work were accomplished under a Phase II STTR DoD award; the views expressed in this paper are not intended as an endorsement by the funding agency. Subject Editor Y. Zohar.

The authors are with mPhase Technologies, Inc., Little Falls, NJ 07424 USA (e-mail: vlifton@mphasetech.com).

Color versions of one or more of the figures in this paper are available online at http://ieeexplore.ieee.org.

Digital Object Identifier 10.1109/JMEMS.2010.2090504

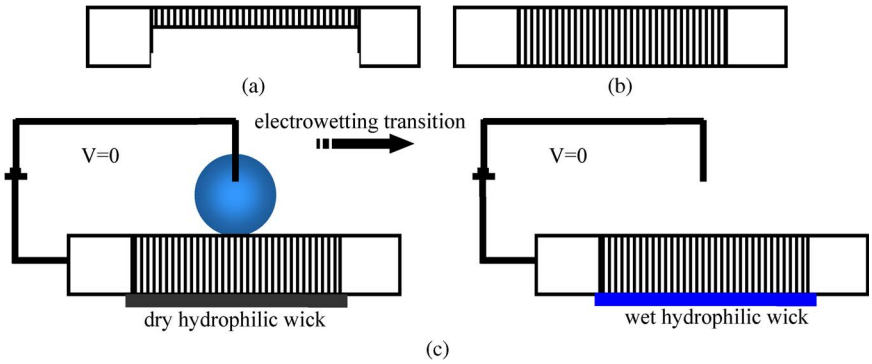

Fig. 1. Comparison of thick and thin membranes (hatched area is the porous area, empty area is the handle/thick Si wafer): (a) not-to-scale cross section through the 30-μm thick SOI membrane and (b) not-to-scale cross section through the 300-μm thick membrane. Schematic depiction of a droplet of liquid sitting on top of the membrane before the electrowetting transition and after the transition, when the liquid is absorbed by a layer of wicking material underneath the membrane.

layer defines the thickness of the membrane (e.g., 30-μm thick) and the handle layer determines the overall thickness (e.g., 300 μm). Fig. 1(a) and (b) show a schematic cross section through the SOI and thick Si membranes. Fig. 1(c) represents a process of electrowetting that will be discussed in more details in Section II-D.

In the SOI-based process, a photolithography step, followed by the through-wafer deep reactive-ion etching (DRIE), formed the pores of the membrane. The backside (handle) layer was also etched to expose the buried oxide and when it was subsequently etched, a thin porous membrane was produced, surrounded by a thick frame (device + handle thickness). The SOI membranes having these characteristics have been integrated into microfluidic reserve microbatteries and are sufficiently robust to survive limited handling, including dip coating and assembly procedures [18]–[20]. The pores investigated were in the 10–40 μm range, with the walls separating adjacent pores $\sim$1-μm wide. We note that porous silicon can also be prepared electrochemically but it does not offer the same degree of control over the size and uniformity across the substrate as photolithography/DRIE process provides.

In the aforementioned design, we also implemented a so-called "nanonail" feature, which imparts superlyophobic properties to the hydrophobic membrane [11]. Without such features, the membrane supports only high-surface-tension liquids. However, by adding the overhang feature, we produced a structure that supports a wide range of liquids, from water to ethanol and hexane, with the surface tension from 72 to 18 mN/m. The essence of this method is the creation of surface structures that set the energy barrier for transitioning from metastable Cassie–Baxter (rolling ball) state, to a stable Wenzel (fully wetted) state, sufficiently high to prevent the transition and to effectively pin the liquid in the desired nonwetting state. Visually, the top surface of the membrane is fabricated to have an overhang lip protruding inside the pore, with the overhang feature creating a re-entrant structure that pins the liquid in the metastable nonwetting state that prevents it from wetting the surface and entering the pores. We typically used silicon nitride as the structural layer to form the overhang by undercutting the Si substrate underneath it.

However, several drawbacks still exist. Since the membranes are only 30-μm thick, they are easily damaged by sharp objects such as tweezers or even fingers during handling, as well as by the smallest pressure if it is applied directly to the membrane and not to the thick silicon frame (e.g., by air pressure during blow drying). The SOI membranes tend to sag under their own weight and particularly when a droplet of liquid is placed on top of it. Preparation of large-area membranes is complicated by the stress in the overhang layer that tends to buckle and ultimately break the membranes during backside etch or buried oxide release step. Such fragility prevents their wider integration into the microbatteries or other applications, particularly those subjected to high acceleration levels and shock environments.

To alleviate these fragility issues, we set on to develop mechanically robust Si structures to create membranes with the uniform thickness across the entire wafer. As an example, we envisioned a membrane 300-μm thick, with the porous region having the same thickness as the silicon frame surrounding it, prepared on a 300-μm thick wafer [Fig. 1(b)]. The structure presented below can be thought of as an extension of the SOI-based approach, with the added advantage of providing significantly improved mechanical robustness of the membranes.

II. Experimental Section

A. Membrane Fabrication

We created a process based on the regular (non-SOI) Si wafers that produces 300-μm thick membranes, with the die size from 18 $\times$ 18 mm to 30 $\times$ 30 mm and porous regions from 5–10 mm on a side, including single and multiple regions on the same die (see Fig. 2 for a brief outline of the process). The size of the porous region is not a limiting factor, and in this paper, it was dictated by the footprint required for our target application. The uniformity of the DRIE process was maintained repeatedly across the entire 6-in wafer. The process starts by using an off-the-shelf thinned silicon wafer followed by the deposition silicon nitride that forms the overhang layer; 70-nm thick in most of the experiment described here. Next, DRIE processing follows the photolithography, to form the pores (Figs. 2 and 3). Using our process, the silicon nitride overhang is formed as a result of controlled undercutting of the silicon nitride layer on the Si wafer (that is, Si substrate immediately underneath SiN is etched away to a certain depth, creating an overhanging SiN structure). Our results indicated that overhangs of various lengths could be formed by carefully monitoring the length of time during the etching steps, along

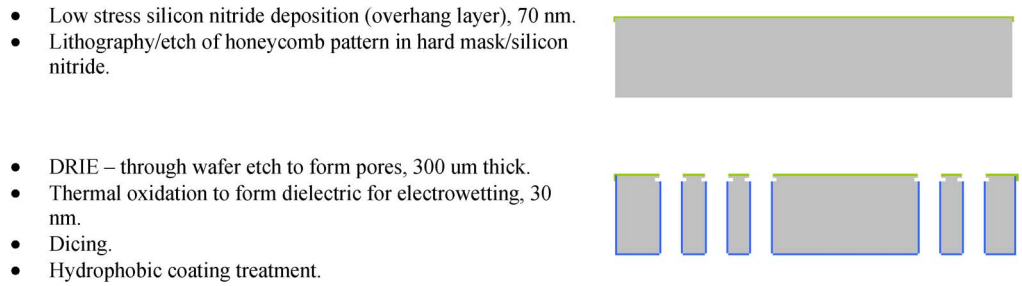

Fig. 2. Outline of the process flow for thick Si membranes. For a detailed discussion of the nanonail geometry, see [11].

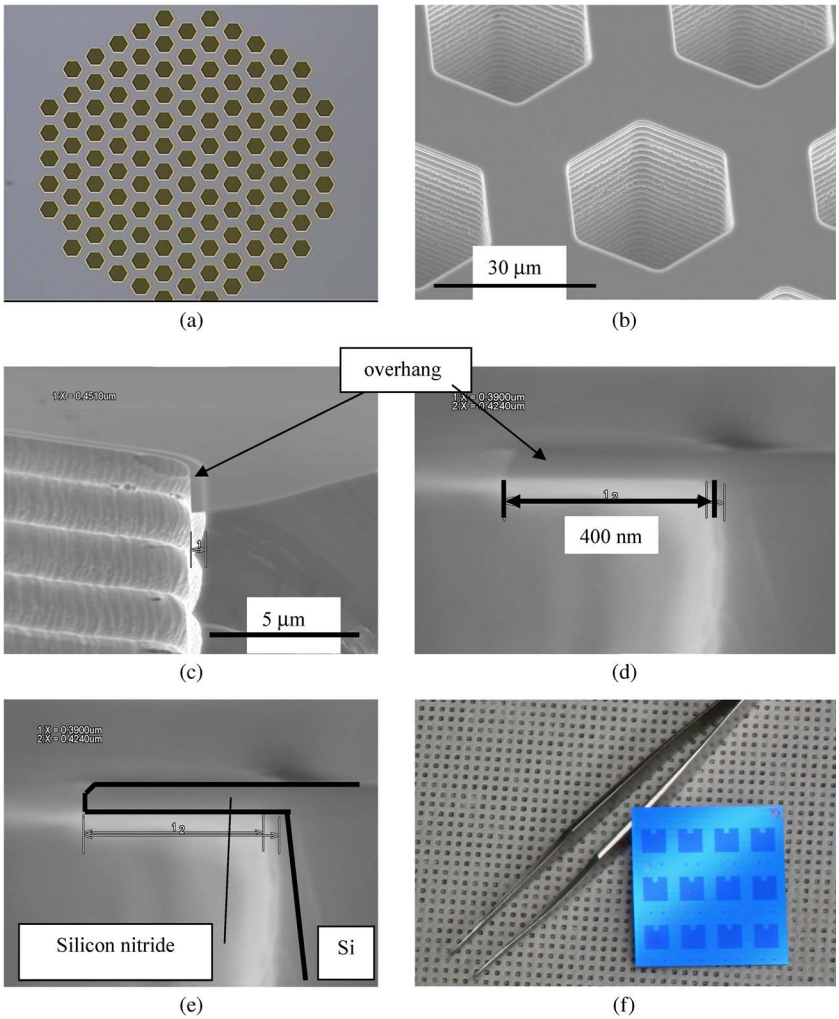

Fig. 3. (a) Optical and (b) SEM photographs of the membrane; (c) and (d) show the details of the overhang structures; (e) is the same image as (d) with the overhang outlined for easier viewing; (f) Photograph of a multicell porous membrane, 30 × 30 mm in size, 300-μm thick, each porous region is 5 × 5 mm.

with careful cycle control of passivation/etching. We found that the longer the overhang, the more stable the structure is against being wetted by a liquid.

Based on our previous experience, we decided to keep the pore size fixed at 30-μm in diameter and varied the width of walls separating adjacent pores. The reason to keep the walls as narrow as possible is to minimize the solid–liquid area of contact, to make sure the surface behaves as a superhydrophobic surface after being treated with a hydrophobic layer. Although we achieved wall widths as narrow as 0.8 μm in our previous work using thin SOI-based membranes, for simplicity of processing, we decided against using such narrow walls on the thick membranes. Therefore, widths of 5, 8, 10, 12, 15, and 20 μm have been investigated. Practically, we found that the widths less than 10 μm do not reliably survive the DRIE etch on the thick 300-μm membranes, so we narrowed down the selection to 12 and 15 μm; where 20-μm walls were deemed unnecessarily wide. Typically, when the wall is formed during the etching step, it may be completely etched or it may be severely overetched deep inside the pore's thickness, making it impossible to determine if there was a successful etch by visual observation from the outside of the structure. Only upon

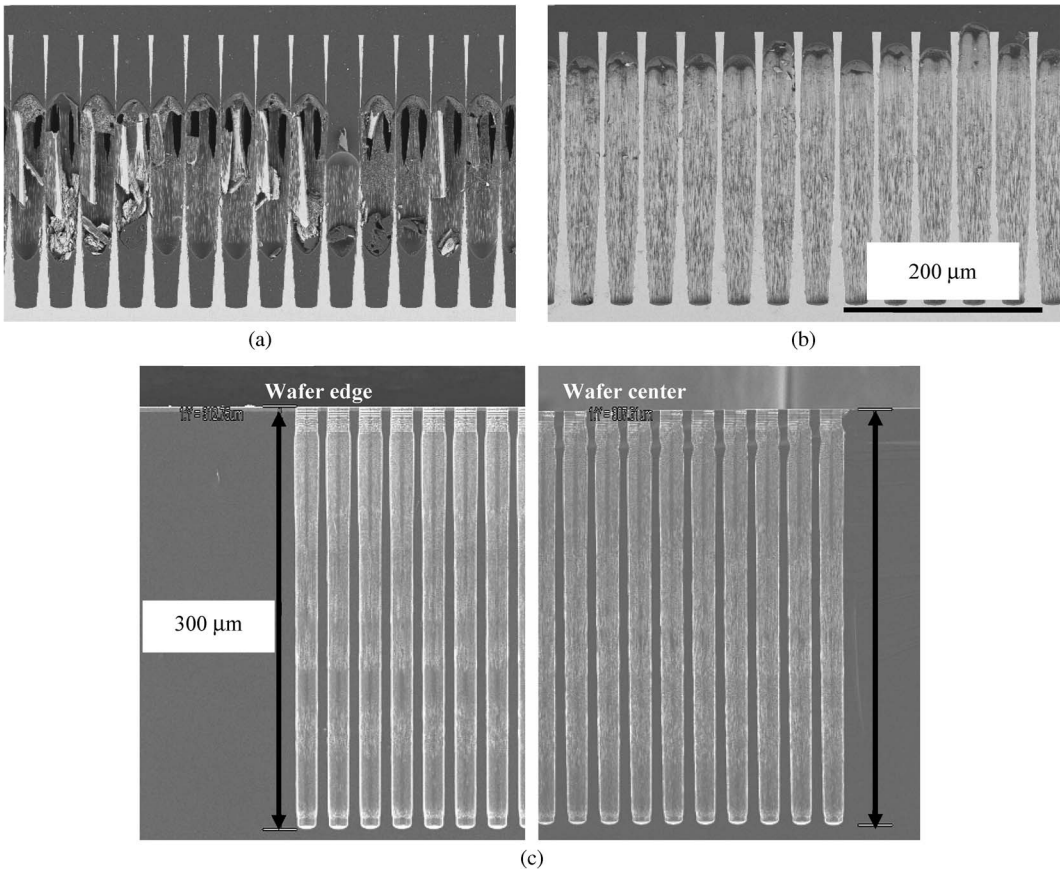

Fig. 4. Cross section through the etched wafers. (a) 10-μm wide walls; (b) 12-μm walls and (c) 15-μm walls. Notice damaged walls inside the sample with 10-μm walls. Using 15-μm walls allows for creation of more uniform walls throughout the thickness.

cross-sectioning, these structures could it be determined if the thru-holes connecting adjacent pores have been formed (Fig. 4). Clearly, this structural condition is unacceptable from the device performance point of view and thicker walls must be used, e.g., 15 μm. Even though wall widths of 10 and 12 μm can be created, the process remained poorly controlled, often resulting in the damaged walls, so that we further narrowed down our selection to the walls 15-μm wide, and in the following discussion, we present the results based on this type of the membrane, unless noted otherwise. As seen in Fig. 4(c), using wider walls helps achieve much more uniform wall width throughout the entire thickness of the membrane. Another manifestation of the poorly tuned DRIE process is significant narrowing of the pore size on the exit (bottom) side of the membrane. In our initial tests, we have seen narrowing pores from 30 μm on the front side to 10–15 μm on the backside, resulting in significantly wider walls on that side [Fig. 4(a) and (b)]. In addition to single membrane cells, we prepared multimembrane samples, with up to 12 individual membranes on a single sample [Fig. 3(f)]. From the processing point of view, there is no difference in processing single or multimembranes.

Thermal oxidation was performed as the last wafer-level step in order to grow a uniform, pin-hole-free SiO_2 dielectric layer 30 nm thick. A dielectric is not required to achieve superlyophobic behavior but was prepared for the follow-up tests on controllable permeability using electrowetting. The significance of the dielectric is well known in studies dealing with the electrowetting transition (often referred to as "electrowetting on dielectric") [6], [21]–[23]. The effect of the dielectric thickness on the trigger voltage for electrowetting on thin SOI Si membranes has been discussed in our previous report [17].

The final step in processing after DRIE, thermal oxidation, and dicing is to coat the samples with a hydrophobic coating, to render them superhydrophobic. Thickness and uniformity of the deposited coating are critical that it should not plug up the pores after coating. We dip coated using 1 and 3 wt. % solutions of Teflon AF 1600; fluoropolymer solutions provided by Cytonix LLC, as well as Repellix vapor-deposited silane-based coatings developed by Integrated Surface Technologies. Dip coating was performed using a bench-top dip coater, TL0-01 (MTI Corp), at 0.1 mm/s pulling speed. The Teflon films were then dried in an oven at 200 °C for 2 h in nitrogen atmosphere. Cytonix coatings were dip coated using the same parameters and air dried at 130–160 °C depending on the type of the coating as specified by the manufacturer. Vapor-deposited coatings were used unmodified as deposited by the provider. All methods appear to provide thin uniform coatings, approximately 100–500-nm thick. We have investigated dip-coated membranes in SEM and have not seen any evidence of pore closing or narrowing as a result of the polymer coating the inner walls of the structure. The vapor-deposited coatings, provided by Integrated Surface Technologies, consist of a network of ceramic nanoparticles, held together by a special linker chemistry and overcoated with a thin layer similar in properties (including wettability and

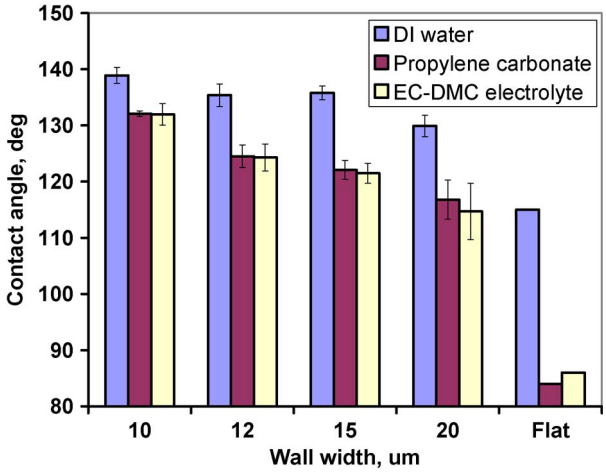

Fig. 5. Contact angle of various liquids as a function of the membrane wall width. Contact angle on the flat surface is given for comparison. Surface tension of water is 72 mN/m, propylene carbonate 42 mN/m, EC-DMC electrolyte 33 mN/m.

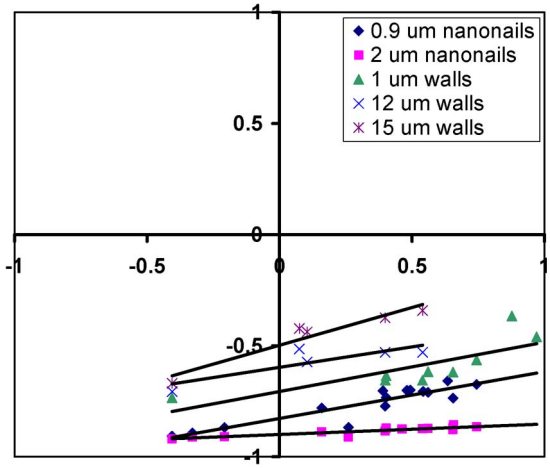

Fig. 6. "Cos-cos" wetting-non-wetting diagram for porous Si membranes showing cosine of the contact angle of the membrane versus cosine of the contact angle on the flat surface treated with the same hydrophobic coating. Data for nanonail structures are shown for comparison (taken from [11]).

contact angle) to fluorinated silane self-assembled monolayers. The differentiating factor in choosing the coating is the reliability or longevity of the coating when in a prolonged contact with the liquid, which is subject of the Section II-C.

Qualitatively, we compared mechanical robustness of the thick membranes and the thin SOI membranes using a well-known approach in the thin film community called a "Scotch tape" peel test. On several samples, we covered porous regions with a Scotch tape (or sometimes Kapton tape) and then pulled the tape off the samples. Thin SOI membranes were always sheared off and damaged in these tests, whereas thick membranes always remained intact even after repeated pull off tests, thus highlighting their increased robustness.

B. Contact Angle Characterization

Contact angle measurements have been performed using VCA Optima XP system (by AST Products, Inc.). In a typical measurement, at least three 5-μl droplets were dispensed and measured.[1] We used both aqueous and organic liquids to examine a wide range of surface tensions. Fig. 5 shows measured contact angles of various liquids on the membranes of various wall widths. There is a clear correlation between the wall width and the contact angle, with the trend toward higher contact angles on the narrower walls. This observation is related to the amount of the solid surface–liquid interface and with the wider wall, more solid area is available for contact, reducing the contact angle toward that on the flat surface treated with the same coating. However, even with the 15-μm wide walls, the air–liquid interface still dominates and the surface behaves as a superhydrophobic/superlyophobic surface. The contact angles for the flat surfaces are given for comparison. Clearly, except for the water, the rest of the low-surface-tension liquids easily wet the flat samples as seen by the contact angle of less than 90 deg. Whereas, the contact angle is reduced on the samples with the wider walls, the droplets of the low-surface-tension liquids are nonetheless supported by the overhang structure, confirming its effectiveness. Note, when a liquid is not supported by the membrane, it would not only spread on the surface but would also permeate through the thickness of the membrane and reach the backside. In a manner consistent with other works dealing with the subject of omniphobic surfaces, we present our contact angle data on a chart showing "cos-cos" relationship, where "cos" corresponds to a cosine of the contact angle on the omniphobic surface and on the corresponding flat surface, Fig. 6. The data forms an approximately linear relationship similar to those given in [12], [24].

In contrast with our previous work, shorter overhang structures are somewhat less stable against the liquids with very low surface tensions, such as hexane and alcohols, as seen by a reduced contact angle on the membrane surfaces (Table I). In fact, most of the structures described in this paper are wetted by alcohols and hexane (surface tension lower than ~25 mN/m). However, it is important to keep in mind that this particular overhang

TABLE I
CONTACT ANGLE OF LIQUIDS ON THE MEMBRANES OF VARYING WALL WIDTHS AND OVERHANG LENGTHS WITH TEFLON AF AS A HYDROPHOBIC COATING

Liquid	Surface tension, (mN/m)	Planar substrate contact angle (degrees)	Contact angle on the membranes with various wall widths and overhang lengths (degrees) (wall width/overhang length)		
			1 µm 500 nm	12 µm 200 nm	15 µm 200 nm
1-octanol	27.60	57.3 72[b]	131	122 114[b]	110
Cyclopentanol	32.70	66.5 84[b]	131	122 145[b]	112
EC-DMC electrolyte	33.1	85.7 147[b]	131	121 160[b]	115
Propylene carbonate[a]	41.90	84 150[b]	132	125 155[b]	116
Water	72.75	113.9 >150[b]	137	135 >160[b]	132 >160[2]

[a] Typical solvent for Li/MnO_2 battery electrolytes.
[b] Using Repellix nanostructured hydrophobic coating from Integrated Surface Technologies.

[1] Unless noted otherwise, values for the advancing contact angle are reported here.

structure has been designed for compatibility with the liquids of certain surface tension (30–40 mN/m) that are used as the electrolytes in Li-based batteries and for the ease of undergoing electrowetting transitions. Experimentally, we determined that 100–300-nm long overhangs provide the optimal performance from the liquid repellency and electrowetting transition points of view. Longer overhangs ($>$ 500 nm) tend to offer high repellency, but adversely require very higher voltages for electrowetting triggering that typically exceeds voltages of the dielectric breakdown of the materials used in fabrication of these membranes. Table I summarizes contact angles of various liquids on the membranes with various overhang lengths and wall widths.

We note that the contact angle on the 15-μm wall width membranes using DI water is about 132°, lower than on the nanonail structures described in [11] (e.g., 157° on the nanonail surface and 137° on 0.8-μm wide wall membrane). This result is related to the area taken by the solid surface (walls), which is in this situation is greater than on the sample with 0.8-μm wide walls or the nanonail structures alone. However, by using specially formulated hydrophobic coatings that contains nanoparticles (e.g., Repellix, provided by Integrated Surface Technologies, Inc.), we demonstrated contact angles on the membranes in excess of 160° and negligible contact angle hysteresis of the high-surface-tension liquids. Here, nanoparticles provide extra features to further reduce the "liquid–solid" interface required to exhibit superhydrophobic behavior. There is a limit to the effectiveness of this approach given a particular solid surface area after which optimization of the re-entrant geometric structures is required, e.g., further minimization of the wall width separating adjacent pores [25]. At the same time, using such novel coatings in conjunction with the nanonail structures offers a high level of flexibility in processing.

C. Long-Term Stability of Hydrophobic Coatings in Electrolytes

Contact angle measurements give a convenient and accurate way to characterize the stability of the coatings on solid surfaces. We used these measurements to monitor any potential degradation of the superhydrophobic properties of the membranes when subjected to long-term exposure to various liquids. Such measurements are important in our work, as these membranes are used as triggerable barriers in the reserve microbattery architecture. These reserve batteries are used when long-term storage is advantageous, with the added requirement of the optimal performance even after a prolonged storage. The porous membrane in this case acts as a separator, restricting the liquid electrolyte from contacting the solid electrode materials. The electrowetting trigger is then used as the external event to allow for the electrolyte to flow through the membrane and initiate the electrochemical reaction to generate voltage. Since the battery is expected to remain in the inactive state for 10–20 years, the superhydrophobic membrane is expected to be exposed to the electrolyte for this period of time and is required to maintain its superhydrophobic properties, as well as to prevent self-triggering and premature failure. Hence, we elected to use contact angle measurements as a way to monitor and predict long-term reliability of the membranes in direct contact with the various electrolytes used in Li-based batteries. We prepared a number of flat and porous membrane samples, coated them with various coatings and immersed them into the electrolyte and periodically measured the contact angle of DI water on such surface. In some instances, to accelerate the ageing processes, we kept the electrolyte temperature at 60 °C.

In Fig. 7(a), we show these tests performed on the first generation of devices that were based on Zn/MnO_2 battery chemistry that uses aqueous $ZnCl_2/NH_4Cl$ electrolyte. Teflon coatings seem to perform the best compared to other fluoropolymers (CYTOP) and self-assembled monolayers for the accumulated exposure time of over 1 year. We attempted to improve the adhesion of Teflon to the substrate using often-employed silane treatment but it had an opposite effect on the stability. Fig. 7(b) shows a snapshot of the follow-up measurements performed over a period of several months, accumulating continuous exposure time of 200 days to the organic electrolyte. The electrolyte specially formulated for our battery work was 1M $LiClO_4$ in 1:1 EC-DMC (ethylene carbonate-dimethyl carbonate). It was chosen for its performance across a wide temperature range, as well as compatibility with the Si-based materials used to prepare superhydrophobic membranes. More commonly used $LiPF_6$ salt was found to be a detrimental component in the electrolyte due to its dissociation and reaction with moisture to produce HF that aggressively etched away SiO_2 and SiN layers. We found that even traces of moisture adsorbed in the surface of the membrane were sufficient to produce enough HF to cause quick degradation in the surface quality. Therefore, we replaced it with $LiClO_4$. Teflon coatings offer an excellent stability over other hydrophobic coatings (the majority of the coatings we tested failed and are not shown here). Contact angle tends to drop after the initial exposure and stabilize around 120–130°. Generally speaking, dip coatings of Teflon and other fluoropolymers showed better long-term stability than vapor deposited coatings such as self-assembled monolayer (these coatings failed after 10–30 days of exposure). Consequently, we excluded self-assembled monolayers from further testing. However, in the situation where only intermittent or short-term exposure to the liquids is expected, such coatings may in fact be preferred, given their ease of deposition from vapor phase. In addition, for many microelectromechanical systems (MEMS) devices, vapor deposition is preferred over dip coatings, as a way to prevent stiction via capillary bridges formed in between delicate structures during dip coating. Our application requirements are to some extent unique and put additional strain on any hydrophobic coating, requiring it to retain its properties for decades of continuous exposure.

At present, we can only speculate on the exact mechanism of degradation, as additional spectroscopic studies such as FTIR and Raman are required to pinpoint the processes leading up to a failure (decrease in the contact angle below 90°). Nevertheless, we offer a hypothesis that given very small thickness of the coatings used in this paper, water molecules (in the case of aqueous electrolytes) diffuse through open structure of amorphous Teflon films and slowly hydrolyze adhesive bonds between the solid substrate (SiO_2 or SiN_x) and Teflon [26]–[28]. We speculate that the adhesion between the substrate and the coating will then slowly decrease outwards, moving along

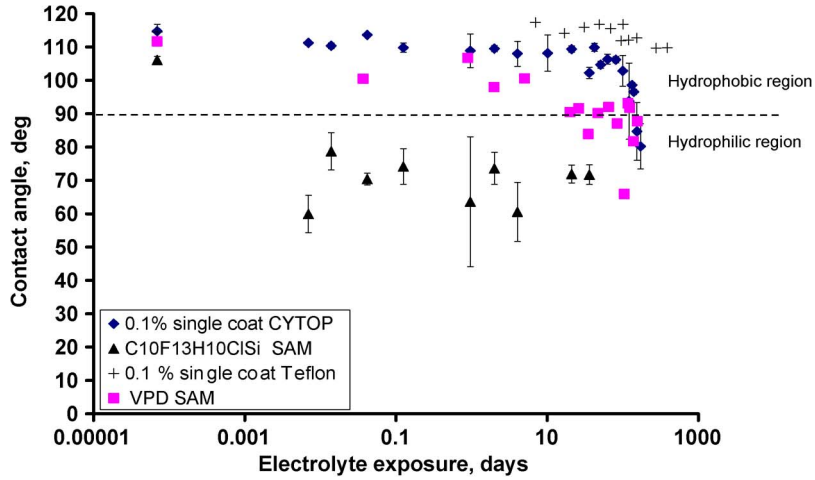

(a)

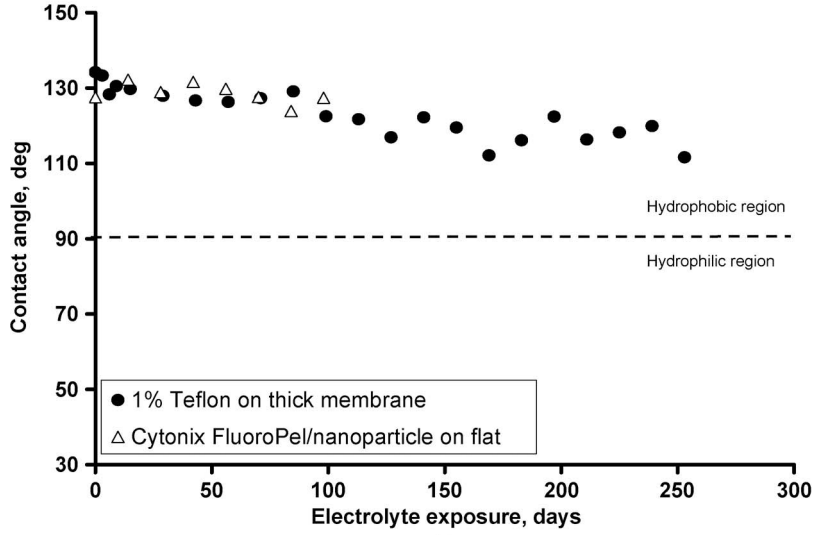

(b)

Fig. 7. (a) Contact angle of DI water on the flat surfaces treated with various hydrophobic coatings as a function of immersion time into aqueous electrolyte based on $ZnCl_2/NH_4Cl$ at room temperature. VPD refers to the self-assembled monolayer deposited via "vapor phase deposition." (b) Contact angle of DI water on various hydrophobic coatings as a function of immersion time into organic EC-DMC electrolyte at 60 °C. Cytonix coating is based on the nanoparticles suspension in a fluoropolymer (FluoroPel M1604V-FS). Notice that even on the flat substrate, it allows to achieve high values of the contact angle.

the interface, forming hydrophilic (wettable) islands, which is indirectly supported by our observation that the degradation always proceeds from the isolated spots and spreads out until the entire surface appears free of coating and is tested hydrophilic. Clearly, surface defects and unintentional scratches will provide the initiation spots; therefore, care must be taken to avoid excessive handling of the coated samples. At the same time, our repeated measurements on the same samples taken over a year worth of tests, confirm their sufficient robustness and reliability. In an application (e.g., microbattery), the membranes will not be subjected to repeated mechanical abrasion through handling and will only experience liquid interface interactions, prolonging their stability.

D. Controllable Permeability of the Membrane Using Electrowetting

To show controllable permeability of the thick membranes, we performed electrowetting tests similar to those described in [17]. Since the electrowetting process is based on the capacitive charging of the solid–liquid interface, no direct dc current flow is required, which leads to a very small energy dissipation during the transition and triggering processes. For example, in our earlier work, we estimated that only ∼60 nJ was dissipated during the trigger process while the battery capacity built with this technology contained at least 1 J. The main reason for energy dissipation is the leakage current through the system due to imperfect dielectric insulators.

Fig. 8 presents photos of the droplet undergoing electrowetting transition. At the end of transition, the droplet is fully absorbed by the wicking material placed underneath the membrane, in contact with the backside of the membrane (see Fig. 1(c) for a pictorial representation of this process). Trigger voltage was in the 70–90-V range, a little higher than previously described in [17]. We believe that it is related to the presence of the overhang structure. In an electrowetting test using regular (no overhang) membrane, the superhydrophobic–hydrophilic transition is initiated immediately upon application of the voltage pulse, whereas in case of the overhang membrane, the first step is the electrostatic attraction of the liquid to the wall

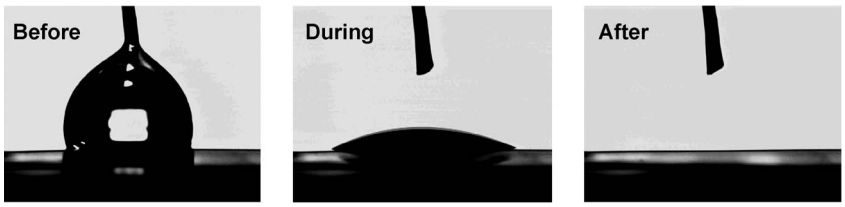

Fig. 8. Photographs of the EC-DMC electrolyte undergoing the electrowetting transition on the surface of superlyophobic membrane treated with Teflon AF. The duration of the transition is on the order of 1–2 s.

directly underneath the overhang, followed by the electrowetting and superhydrophobic–hydrophilic transition. This behavior explains the reason for having overhangs in the certain range (100–300-nm long). The longer the overhang, the higher the voltage needed to induce the electrostatic attraction. However, it can quickly exceed the dielectric strength of the dielectric material that forms the overhang and lead to a dielectric breakdown in the system, after which no electrowetting transition is possible. At the same time, if no electrowetting transitions are required from the system or the application using this technology, the longer overhangs will yield better stability of the liquids on the membranes, without the risk of self-triggering and spontaneous wetting.

As was mentioned in the section describing fabrication of the membrane, one of the steps is processing is thermal oxidation. It is used to create a conformal layer of dielectric over the entire surface of the membrane. Such layer is critical to the observation of electrowetting transitions. Thermal oxide is certainly not the only dielectric that can be used for this purpose but it offers several advantages, such as ease of processing, control of its thickness, and high dielectric strength among other properties. However, its formation occurs at high temperatures, and it may not be a suitable approach for applying a dielectric in cases where the components of the overall structure may contain metals or polymers. In this case, one can conveniently use parylene as a dielectric. Parylene has been widely used as a dielectric of choice in a variety of works dealing with electrowetting and has been shown to be an excellent substitute for SiO_2. We have used deposited parylene over our porous Si membranes and have achieved results similar to those obtained using SiO_2, both in terms of superhydrophobic properties and the trigger voltage for electrowetting transition (50–70 V). The important conclusion from these tests indicated that vapor-deposited coatings (such as parylene) do not change or mask the geometry of the overhang features.

Functionality of the membranes presented in this paper may be compared to the other tunable surfaces using electrowetting, see [6], [29] for a review of recent work on this subject. Several groups have reported on tunable wetting of various surfaces sensitive to heat, illumination, or a change in pH. As reported in these works, a change in external stimulus led to a change in wetting properties of a solid surface. Demonstrated reversibility of such response should also be noted. However, we must point out that in the majority of these cases the response was confined to the surface of the material, whereas in this paper, we present a way to change the response of the material not only on the surface but also throughout its thickness, resulting in dynamically controllable permeability of the material.

III. Potential Applications of Si-Based Membranes

We envision several applications for such superlyophobic membranes. One has already been described and is actively pursued by our group in the reserve microbattery technology [18]–[20]. Currently, prototype Li/MnO_2 batteries are being tested. Images on Fig. 9 show schematic of the existing battery prototype, as well as the location of the superlyophobic membrane in the battery. The membrane built for this application contains 12 individual membranes, each one corresponding to an electrochemical cell, thus forming an array of 3×4 power cells in a single battery substrate (Fig. 3(f) shows a single 3×4 membrane die). Each cell is designed to provide enough capacity to last for approximately 3 years under the projected current draw. Upon reaching its end-of-life, the next cell will be triggered for a combined total capacity of approximately 30-year active life for this application. Since only one cell at a time is active (electrolyte is in contact with the electrodes), the rest of the cells remain in the inactive (hence, the name reserve) state, without self-discharge and unwanted chemical reactions that would normally limit the active life to only 10 years.

The membranes can be also used as the capillary adhesives described recently in [30]. The basic principle in this approach is the capillary adhesion due to droplets protruding from the backside of the membrane after the electrowetting transition. When brought in contact with another surface, capillary bridges will be formed and the surfaces will be pulled together and held tightly. The electrically triggereable membrane may offer a way to create controlled wetting and even spacing of the adhesive capillary bridges, as well as a way to combine liquids with various surface tension on the same device to address chemical compatibility and stability issues.

On the other hand, given sensitivity of the overhang structure to the surface tension of the liquid, one can imagine using it for filtration or separation of the mixtures or emulsions of the liquids of various surface tensions (oil/water, for example) [3], [16], [31]. Other possibilities are potential uses as water barriers in fuel cells, where liquid water accumulation may poison the fuel cell or reduce its efficiency [32]. In this example, the membranes could potentially prevent water from flowing across and, at the same time, remaining permeable by the vapors to reduce pressure drops in different parts of the system.

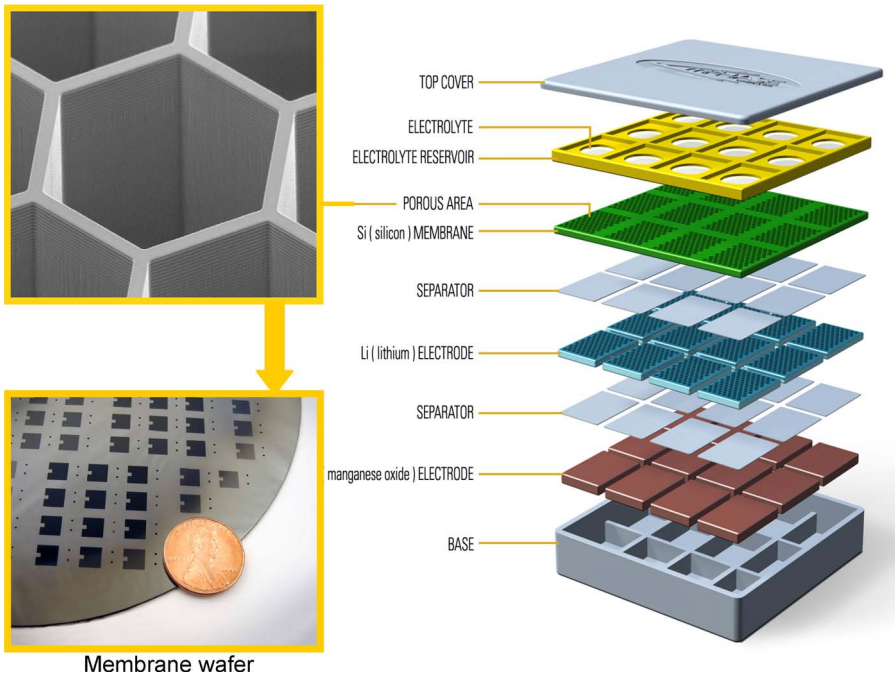

Fig. 9. Schematic of the multicell reserve microbattery. Each cell in the 3 × 4 array is designed to last for 3 years, subsequently triggering the neighboring cell, thus, providing for 30-year life time.

IV. Conclusion

In summary, we described fabrication and testing of the 300-μm thick superlyophobic porous silicon membranes. Rigid structures are produced using a DRIE etching process through the entire wafer thickness (300 μm), which represents a significant improvement over the previously described SOI-based, thin (30 μm) porous membranes. We have demonstrated that the special overhang structures impart superlyophobic behavior onto ordinary hydrophobic surfaces and that controllable permeability of these structures can be accomplished using the electrowetting phenomenon. In addition, we presented reliability studies of various hydrophobic coatings deposited on these membranes subjected to long-term exposure to aqueous and organic battery electrolytes, making that suitable for real-world applications needing longevity. We have also suggested the applicability of such membranes in construction of reserve microbatteries, as well as potential use in filtration, separation, and capillary adhesives designs.

Acknowledgment

Continued support by mPhase Technologies is greatly appreciated.

References

[1] L. B. Boinovich and A. M. Emelyanenko, "Hydrophobic materials and coatings: Principles of design, properties and applications," *Russ. Chem. Rev.*, vol. 77, no. 7, pp. 583–600, 2008.

[2] L. Gao and T. J. McCarthy, "Wetting 101 °†," *Langmuir*, vol. 25, no. 24, pp. 14 105–14 115, Dec. 2009.

[3] A. Tuteja, W. Choi, M. Ma, J. M. Mabry, S. A. Mazzella, G. C. Rutledge, G. H. McKinley, and R. E. Cohen, "Designing superoleophobic surfaces," *Science*, vol. 318, no. 5856, pp. 1618–1622, Dec. 2007.

[4] D. Quéré, "Wetting and roughness," *Annu. Rev. Mater. Res.*, vol. 38, no. 1, pp. 71–99, 2008.

[5] P. Roach, N. J. Shirtcliffe, and M. I. Newton, "Progess in superhydrophobic surface development," *Soft Matter*, vol. 4, no. 2, pp. 224–240, 2008.

[6] J. Heikenfeld and M. Dhindsa, "Electrowetting on superhydrophobic surfaces: Present status and prospects," *J. Adhesion Sci. Technol.*, vol. 22, no. 3, pp. 319–334, 2008.

[7] V. A. Lifton and S. Simon, "Wetting the surface: From self-cleaning leaves to energy storage devices," in *Bionanotechnology: Global Prospects*, D. Reisner, Ed. Boca Raton, FL: CRC Press, 2009.

[8] T. N. Krupenkin, J. A. Taylor, T. M. Schneider, and S. Yang, "From rolling ball to complete wetting: The dynamic tuning of liquids on nanostructured surfaces," *Langmuir*, vol. 20, no. 10, pp. 3824–3827, May 2004.

[9] H. Lee and J. Owens, "Design of superhydrophobic ultraoleophobic NyCo," *J. Mater. Sci.*, vol. 45, no. 12, pp. 3247–3253, Jun. 2010.

[10] D. Han and A. J. Steckl, "Superhydrophobic and oleophobic fibers by coaxial electrospinning," *Langmuir*, vol. 25, no. 16, pp. 9454–9462, Aug. 2009.

[11] A. Ahuja, J. A. Taylor, V. Lifton, A. A. Sidorenko, T. R. Salamon, E. J. Lobaton, P. Kolodner, and T. N. Krupenkin, "Nanonails: A simple geometrical approach to electrically tunable superlyophobic surfaces," *Langmuir*, vol. 24, no. 1, pp. 9–14, Jan. 2008.

[12] S. S. Chhatre, W. Choi, A. Tuteja, K.-C. Park, J. M. Mabry, G. H. McKinley, and R. E. Cohen, "Scale dependence of omniphobic mesh surfaces," *Langmuir*, vol. 26, no. 6, pp. 4027–4035, Mar. 2010.

[13] V. A. Lifton and S. Simon, "Preparation and electrowetting transitions on superhydrophobic/hydrophilic bi-layer structures," *J. Porous Mater.*, 2010. DOI: 10.1007/s10934-010-9406-0.

[14] B. Balu, V. Breedveld, and D. W. Hess, "Fabrication of 'Roll-off' and 'Sticky' superhydrophobic cellulose surfaces via plasma processing," *Langmuir*, vol. 24, no. 9, pp. 4785–4790, May 2008.

[15] B. Balu, J. S. Kim, V. Breedveld, and D. W. Hess, "Tunability of the adhesion of water drops on a superhydrophobic paper surface via selective plasma etching," *J. Adhesion Sci. Technol.*, vol. 23, no. 2, pp. 361–380, 2009.

[16] A. Tuteja, W. Choi, J. M. Mabry, G. H. McKinley, and R. E. Cohen, "Robust omniphobic surfaces," *Proc. Nat. Acad. Sci.*, vol. 105, no. 47, pp. 18 200–18 205, Nov. 2008.

[17] V. A. Lifton, J. A. Taylor, B. Vyas, P. Kolodner, R. Cirelli, N. Basavanhally, A. Papazian, R. Frahm, S. Simon, and T. Krupenkin, "Superhydrophobic membranes with electrically controllable permeability and their application to 'smart' microbatteries," *Appl. Phys. Lett.*, vol. 93, no. 4, p. 043 112, Jul. 2008.

[18] V. A. Lifton, S. Simon, and R. E. Frahm, "Reserve battery architecture based on superhydrophobic nanostructured surfaces," *Bell Labs Tech. J.*, vol. 10, no. 3, pp. 81–85, 2005.

[19] V. A. Lifton, S. Simon, and F. M. Allen, "A chemistry-independent microbattery with enhanced functionality," in *Proc. NSTI*, 2008, pp. 467–470.
[20] V. A. Lifton and S. Simon, "Micro scale addressable superhydrophobic reserved batteries using nanostructured materials," in *Proc. 42nd Power Sources Conf.*, Jun. 2006, pp. 1–4.
[21] F. Mugele and J. Baret, "Electrowetting: From basics to applications," *J. Phys., Condens. Matter*, vol. 17, no. 28, pp. R705–R774, Jul. 2005.
[22] H. Liu, S. Dharmatilleke, D. K. Maurya, and A. A. O. Tay, "Dielectric materials for electrowetting-on-dielectric actuation," *Microsyst. Technol.*, vol. 16, no. 3, pp. 449–460, 2009.
[23] E. Seyrat and R. A. Hayes, "Amorphous fluoropolymers as insulators for reversible low-voltage electrowetting," *J. Appl. Phys.*, vol. 90, no. 3, pp. 1383–1386, Aug. 2001.
[24] S. M. M. Ramos, A. Benyagoub, B. Canut, and C. Jamois, "Superoleophobic behavior induced by nanofeatures on oleophilic surfaces," *Langmuir*, vol. 26, no. 7, pp. 5141–5146, Apr. 2010.
[25] E. Lobaton and T. Salamon, "Computation of constant mean curvature surfaces: Application to the gas-liquid interface of a pressurized fluid on a superhydrophobic surface," *J. Colloid Interface Sci.*, vol. 314, no. 1, pp. 184–198, Oct. 2007.
[26] A. Tokarev, K. Friess, J. Machkova, M. Scaronipek, and Y. Yampolskii, "Sorption and diffusion of organic vapors in amorphous Teflon AF2400," *J. Polym. Sci. B, Polym. Phys.*, vol. 44, no. 5, pp. 832–844, Mar. 2006.
[27] A. Polyakov, G. Bondarenko, A. Tokarev, and Y. Yampolskii, "Intermolecular interactions in target organophilic pervaporation through the films of amorphous Teflon AF2400," *J. Membrane Sci.*, vol. 277, no. 1, pp. 108–119, Jun. 2006.
[28] I. Pinnau and L. G. Toy, "Gas and vapor transport properties of amorphous perfluorinated copolymer membranes based on 2,2-bistrifluoromethyl-4,5-difluoro-1,3-dioxole/tetrafluoroethylene," *J. Membrane Sci.*, vol. 109, no. 1, pp. 125–133, Jan. 1996.
[29] N. Verplanck, Y. Coffinier, V. Thomy, and R. Boukherroub, "Wettability switching techniques on superhydrophobic surfaces," *Nanoscale Res. Lett.*, vol. 2, no. 12, pp. 577–596, Dec. 2007.
[30] M. J. Vogel and P. H. Steen, "Capillarity-based switchable adhesion," *Proc. Nat. Acad. Sci.*, vol. 107, no. 8, pp. 3377–3381, Feb. 2010.
[31] S. S. Chhatre, A. Tuteja, W. Choi, A. Revaux, D. Smith, J. M. Mabry, G. H. McKinley, and R. E. Cohen, "Thermal annealing treatment to achieve switchable and reversible oleophobicity on fabrics," *Langmuir*, vol. 25, no. 23, pp. 13 625–13 632, Dec. 2009.
[32] T. Metz, J. Viertel, C. Müller, S. Kerzenmacher, N. Paust, R. Zengerle, and P. Koltay, "Passive water management for μfuel-cells using capillary microstructures," *J. Micromech. Microeng.*, vol. 18, no. 10, p. 104 007, Oct. 2008.

Victor A. Lifton (M'96) received the M.S. degree from Moscow Institute of Steel and Alloys, Moscow, Russia, in 1993, and the Ph.D. degree in materials science and engineering from Stevens Institute of Technology, Hoboken, NJ, in 1999.

From 1999 to 2004, he held various R&D positions in semiconductor processing and MEMS fabrication at Measurement Specialties, Inc., Kulite Semiconductor Products, and Bell Laboratories. In 2004, he joined mPhase Technologies, Little Falls, NJ, as a Senior Member of Technical Staff, and in 2006, he became Chief Scientist. His current job responsibilities include basic and applied R&D activities in the company's efforts in nanotechnology and commercialization of nanotechnology-based products such as reserve microbatteries.

Steve Simon (M'97) received the B.A. degree in multimedia productions from New York University, New York, NY, and the M.S. degree in computer science from the City College of New York, New York, NY.

He is Executive Vice President for Research and Development of mPhase Technologies Inc., Little Falls, NJ. He is responsible for managing the research and development of mPhase's portfolio of nano- and MEMS-based products. Prior to joining mPhase Technologies, he held positions as a Distinguished Member of Technical Staff and Technologies Consultant at AT&T Labs and Lucent Bell Labs. He is the holder of six patents in the telecommunications and nanotechnology areas.

Mr. Simon was awarded the Frost and Sullivan 2005 award for company innovation for bringing a novel nanobattery to the marketplace.